# Bethe-Peierls approximation with competing order parameters*

E. Eggarter and T. P. Eggarter
*Departamento de Fisica, Universidad Nacional de San Luis, 5700 San Luis, Argentina*
(Received 20 August 1975)

We study an alloy of Ising spins between a ferromagnetic and an antiferromagnetic species. Pairs of $AA$, $AB$, and $BB$ neighbors are characterized by different coupling constants $J_{AA}$, $J_{AB}$, and $J_{BB}$. Our approach is based on a generalization of the Bethe-Peierls approximation to the case of compositional disorder. We find a phase diagram with a bicritical or tetracritical point depending on the strength of the coupling $J_{AB}$ between species.

## I. INTRODUCTION

The Ising model on a perfect lattice has a long history[1]; several hundred articles on this subject have been written. It has greatly contributed to our understanding of magnetism and of phase transitions in general. Much less is known about the model if the periodicity of the lattice is destroyed by compositional or topological disorder. Fan and McCoy[2] have studied the bidimensional model with small random fluctuations in the coupling constants, and Lee, Montroll, and Yu[3] worked out an exact solution for the one-dimensional binary alloy. One of us[4] has extended the Bethe-Peierls approximation to an alloy with an arbitrary number of components assuming all $J_{ij}$'s to be positive. The purpose of this paper is to study, within the same approximation, an alloy between a ferromagnetic and an antiferromagnetic species. Wissel[5] and Wegner[6] have studied this problem in the molecular-field (or mean-field) approximation. It has also been considered from a different point of view by Bruce and Aharony,[7] who studied critical exponents for systems with several coupled order parameters. The kind of information obtained in the two approaches is complementary: mean-field theory aims at giving the global characteristics of the phase diagram, including explicit equations for the various critical lines in terms of coupling constants and concentrations, but is unable to give the correct critical behavior. Renormalization-group techniques, on the other hand, give accurate information about critical exponents, but the explicit dependence of $T_c$ on the parameters of the initial Hamiltonian gets buried in the renormalization transformations.

Our work is a more elaborate treatment of the problem along the lines of Wissel and Wegner, since the Bethe-Peierls approximation is known to be an improvement over the plain mean-field approximation. Our results are in general in good qualitative agreement with theirs. Some obvious shortcomings of molecular-field theory, like the prediction of a phase transition in one dimension, are corrected in our approach. The main results are the following: depending on the strength of the coupling between species, two kinds of phase diagrams [Figs. 1(a) and 1(b)] are possible in the absence of an external field. For strong coupling $J_{AB}$ between the species [Fig. 1(a)] the system is ferromagnetic at low $T$ if it is sufficiently rich in the ferromagnetic species (which we call $A$), and antiferromagnetic otherwise. The ferromagnetic (FM) and antiferromagnetic (AFM) regions are separated by a line $OC$ of first-order transitions. If the coupling $J_{AB}$ is weak [Fig. 1(b)] the AFM and FM regions are separated by a mixed phase in which both types of order coexist. The intermediate or mixed phase exhibits a splitting into two sublattices $L$ and $L'$ with average magnetizations $\langle\sigma\rangle$ and $\langle\sigma'\rangle$, which are neither equal nor opposite. It arises physically from the fact that the $A$ sites form a dilute ferromagnet interwoven with a dilute antiferromagnet of $B$ sites. This mixed phase has been observed[8] in $Fe(Pd_xPt_{1-x})_3$ and in $(Mn_xFe_{1-x})WO_4$, and it was in connection with these substances that Wissel and Wegner did their mean-field calculations.

In Sec. II of this paper we define our model. The basic equations are derived in III. Their solutions

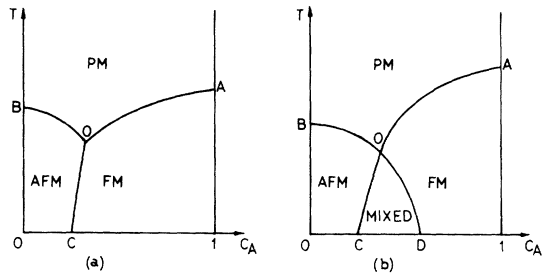


FIG. 1. Phase diagrams for an alloy between a ferromagnetic species $A$ and an antiferromagnetic species $B$ without external field. The regions are indicated as PM (paramagnetic), AFM (antiferromagnetic), FM (ferromagnetic), and mixed; the last one exhibits a superposition of FM and AFM long-range order. Case (a) results if the coupling $J_{AB}$ between species is strong, case (b) if it is weak.

and the resulting phase diagrams are discussed in Sec. IV. Finally, representative results and a comparison with mean-field results are presented in Sec. V and a brief summary is given in Sec. VI.

## II. DEFINITION OF THE MODEL

We consider two kinds of atoms $A$ and $B$ distributed at random on a regular lattice. We assume for simplicity that different sites are statistically independent as far as their occupation by $A$ or $B$ atoms is concerned.[9] The atoms remain frozen in at fixed positions in the lattice, and their concentrations are $c_A$ and $c_B = 1 - c_A$. We postulate a magnetic Hamiltonian of the form

$$H = -\sum_{(i,j)} J_{ij}\sigma_i\sigma_j - h\sum_i g_i\sigma_i, \tag{1}$$

where the $\sigma_i$ are Ising spins $\sigma_i = \pm 1$, the first sum is over all pairs of neighbors, and $J_{ij}$ is $J_{AA}$, $J_{AB}$, or $J_{BB}$ depending on the atoms at sites $i,j$; $h$ is an applied external field, and $g_i$ is $g_A$ or $g_B$, the magnetic moment of the atom at site $i$. We want to work with one species $A$ which is ferromagnetic when pure and another species $B$ which is antiferromagnetic when pure; therefore, $J_{AA} > 0$, $J_{BB} < 0$. We can take $J_{AB} > 0$ without loss of generality since the sign of $J_{AB}$ can be changed at will by transforming $\sigma \to -\sigma$ for one of the species.

To make antiferromagnetism possible we split our lattice into two sublattices $L$ and $L'$ in the usual way: each site in $L$ has all its neighbors in $L'$ and vice versa. We only consider lattices on which such a decomposition is possible, for example, simple cubic or plane hexagonal.

We shall try to determine the probabilities $P(i,\sigma;i',\sigma')$, $i = A$ or $B$, $i' = A$ or $B$, $\sigma = \pm 1$, $\sigma' = \pm 1$, for the occupation and spin configuration at two neighboring sites with the system in thermal equilibrium. We assume that the first pair of arguments in $P$ corresponds to a site in $L$, the second pair to a site in $L'$. A knowledge of the probabilities $P(i,\sigma;i',\sigma')$ at all temperatures and applied fields is sufficient to determine all thermodynamic quantities: the energy is

$$E = \langle H\rangle = -\sum_{i,\sigma,i',\sigma'} P(i,\sigma;i',\sigma')[J_{ii'}\sigma\sigma' + \tfrac{1}{2}(g_i\sigma + g_{i'}\sigma')], \tag{2}$$

and from $E$ all other thermodynamic functions can be obtained using the first and second principles of thermodynamics.

Our aim will be to write down a closed system of equations for the pair probabilities $P(i,\sigma;i',\sigma')$ in the Bethe-Peierls approximation. To do so it will be convenient to define also the single-site probabilities

$$P(i,\sigma) \equiv \sum_{i',\sigma'} P(i,\sigma;i',\sigma'), \tag{3a}$$

$$P'(i',\sigma') \equiv \sum_{i,\sigma} P(i,\sigma;i',\sigma'), \tag{3b}$$

as well as the conditional probabilities

$$P_c(i,\sigma/i',\sigma') \equiv P(i,\sigma;i',\sigma')/P'(i',\sigma'), \tag{4a}$$

$$P'_c(i',\sigma'/i,\sigma) \equiv P(i,\sigma;i',\sigma')/P(i,\sigma). \tag{4b}$$

$P_c(i,\sigma/i',\sigma')$ is the conditional probability that given a site in $L'$ with $i',\sigma'$, a neighboring site in $L$ will be $i,\sigma$. Similarly for $L$ and $L'$ interchanged.

## III. BASIC EQUATIONS

To derive the equations for the $P(i,\sigma;i',\sigma')$ we start by considering an arbitrary site in $L$ together with all its neighbors (Fig. 2). Let $Q(A,\uparrow;n_A,m_A,n_B,m_B)$ be the probability that the central site has $i,\sigma = A,\uparrow$ and that $n_A$ given sites among its neighbors are $A$, $\uparrow$, $m_A$ are $A$, $\downarrow$, $n_B$ are $B$, $\uparrow$, and $m_B$ are $B$, $\downarrow$. We take $n_A + m_A + n_B + m_B = \gamma$, the coordination number. In the spirit of the Bethe-Peierls approximation which replaces the lattice by a Cayley tree[10] of the same coordination, we write

$$\begin{aligned} Q(A,\uparrow;n_A,m_A,n_B,m_B) &= P(A,\uparrow)P'_c(A,\uparrow/A,\uparrow)^{n_A}P'_c(A,\downarrow/A,\uparrow)^{m_A} \\ &\times P'_c(B,\uparrow/A,\uparrow)^{n_B}P'_c(B,\downarrow/A,\uparrow)^{m_B}. \end{aligned} \tag{5a}$$

Suppose now that the central spin is reversed while everything else remains unchanged. Let $Q(A,\downarrow;n_A,m_A,n_B,m_B)$ be the corresponding probability; then

$$\begin{aligned} Q(A,\downarrow;n_A,m_A,n_B,m_B) &= P(A,\downarrow)P'_c(A,\uparrow/A,\downarrow)^{n_A}P'_c(A,\downarrow/A,\downarrow)^{m_A} \\ &\times P'_c(B,\uparrow/A,\downarrow)^{n_B}P'_c(B,\downarrow/A,\downarrow)^{m_B}. \end{aligned} \tag{5b}$$

Let $H_{\text{clust}}$ be the Hamiltonian of the cluster Fig. 2, and $H_{\text{out}} \equiv H - H_{\text{clust}}$. Let $\text{Tr}_{\text{out}}$ stand for the trace over all spin variables outside the cluster. Then from statistical mechanics

$$\begin{aligned} \frac{Q(A,\uparrow;n_A,m_A,n_B,m_B)}{Q(A,\downarrow;n_A,m_A,n_B,m_B)} &= \frac{\exp[-\beta E_{\text{clust}}(A,\uparrow;n_A,m_A,n_B,m_B)]\,\text{Tr}_{\text{out}}[\exp(-\beta H_{\text{out}})]}{\exp[-\beta E_{\text{clust}}(A,\downarrow;n_A,m_A,n_B,m_B)]\,\text{Tr}_{\text{out}}[\exp(-\beta H_{\text{out}})]} \\ &= \exp\{2\beta[hg_A + J_{AA}(n_A - m_A) + J_{AB}(n_B - m_B)]\}. \end{aligned} \tag{6}$$

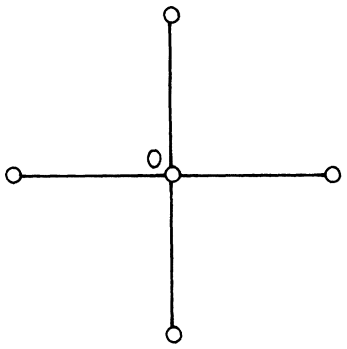

FIG. 2. Cluster considered exactly in the Bethe-Peierls approximation. It consists of a central site 0 and its $\gamma$ nearest neighbors. The figure corresponds to a planar square lattice with $\gamma=4$.

Substituting Eqs. (5) into (6) and using the definition (4) of the conditional probabilities we may write

$$\left(\frac{P(A,\downarrow)}{P(A,\uparrow)}\right)^{\gamma-1}\left(\frac{P(A,\uparrow;A,\uparrow)}{P(A,\downarrow;A,\uparrow)}\right)^{n_A}\left(\frac{P(A,\uparrow;A,\downarrow)}{P(A,\downarrow;A,\downarrow)}\right)^{m_A}$$
$$\times\left(\frac{P(A,\uparrow;B,\uparrow)}{P(A,\downarrow;B,\uparrow)}\right)^{n_B}\left(\frac{P(A,\uparrow;B,\downarrow)}{P(A,\downarrow;B,\downarrow)}\right)^{m_B}$$
$$=\exp\{2\beta[hg_B+J_{AA}(n_A-m_A)+J_{AB}(n_B-m_B)]\}. \tag{7}$$

Similar equations hold of course for $A$ and $B$ interchanged, and for the sublattices $L$ and $L'$ interchanged. [Interchanging $L$ and $L'$ amounts to using $P'(A,\uparrow)$, etc., in the first factor of the left-hand side of (7), and to interchanging the order of the pairs of arguments in the various $P(i,\sigma;i',\sigma')$.] Since the $n_A, m_A, n_B, m_B$ are arbitrary integers which sum up to $\gamma$, there is a large number of equations of the form (7). In addition to all these, the $P(i,\sigma;i',\sigma')$ must also satisfy

$$\sum_{\sigma,\sigma'} P(i,\sigma;i',\sigma')=c_i c_{i'} \tag{8}$$

because of our assumption of a random and frozen-in distribution of atoms.

To find $P(i,\sigma;i',\sigma')$'s satisfying all these conditions we make the ansatz[4]

$$P(i,\sigma;i',\sigma')=c_i c_{i'}\exp(\beta J_{ii'}\sigma\sigma')\exp(u_i\sigma+u'_{i'}\sigma')/D_{ii'}, \tag{9}$$

with

$$D_{ii'}=2[\cosh(u_i+u'_{i'})\exp(\beta J_{ii'})$$
$$-\cosh(u_i-u'_{i'})\exp(-\beta J_{ii'})] \tag{10}$$

and with $u_A, u'_A, u_B, u'_B$ quantities to be determined. The choice (9) and (10) ensures that the set of equations (8) is identically satisfied. Furthermore substitution of (9) into (7) yields

$$[P(A,\downarrow)/P(A,\uparrow)]^{\gamma-1}\exp(2\gamma u_A)=\exp(2\beta h g_A) \tag{11}$$

or

$$u_A=\frac{\gamma-1}{2\gamma}\ln\left(\frac{P(A,\uparrow)}{P(A,\downarrow)}\right)+\frac{hg_A}{\gamma kT}\equiv f_A(u_A,u'_A,u_B,u'_B) \tag{12a}$$

and similar equations for $A\rightleftarrows B$ and for $L\rightleftarrows L'$:

$$u_B=\frac{\gamma-1}{2\gamma}\ln\left(\frac{P(B,\uparrow)}{P(B,\downarrow)}\right)+\frac{hg_B}{\gamma kT}\equiv f_B(u_A,u'_A,u_B,u'_B), \tag{12b}$$

$$u'_A=\frac{\gamma-1}{2\gamma}\ln\left(\frac{P'(A,\uparrow)}{P'(A,\downarrow)}\right)+\frac{hg_A}{\gamma kT}\equiv f'_A(u_A,u'_A,u_B,u'_B), \tag{12c}$$

$$u'_B=\frac{\gamma-1}{2\gamma}\ln\left(\frac{P'(B,\uparrow)}{P'(B,\downarrow)}\right)+\frac{hg_B}{\gamma kT}\equiv f'_B(u_A,u'_A,u_B,u'_B). \tag{12d}$$

We have obtained in this way a closed set of four equations which have to be solved for $u_A, u'_A, u_B, u'_B$. If $h=0$ then $u_A=u'_A=u_B=u'_B=0$ is one possible solution of Eqs. (12). According to (9) this trivial solution corresponds to equal probabilities for spins up or down; it therefore describes a paramagnetic phase. The existence or not of other solutions depends on the values of the parameters and the temperature. If other solutions exist they have to be found in general numerically (representative results will be given in Sec. V). Nevertheless, a fair amount of information can be obtained analytically by studying Eqs. (12) in the vicinity of the critical lines $OA, OB$ of Fig. 1, where the magnetizations, and therefore the $u$'s, are small. Before discussing this subject we make the following observation:

The energy *per bond* obtained from Eq. (2), when expressed in terms of the $u$'s, takes the form

$$E=-\sum_{i,i'}J_{ii'}c_i c_{i'}$$
$$\times\frac{\tanh(\beta J_{ii'})+\tanh(u_i)\tanh(u_{i'})}{1+\tanh(\beta J_{ii'})\tanh(u_i)\tanh(u_{i'})} \tag{13}$$

(we set $h=0$ from now on). For $T\to 0$ it becomes

$$E(T=0)=-\sum_{i,i'}c_i c_{i'}|J_{ii'}|, \tag{14}$$

which is exact on a Cayley tree, but an underestimate of the ground-state energy on a real lattice. Equation (14) implies that every bond is in its state of minimum energy $-|J_{ii'}|$, and this is impossible if closed loops exist. Consider, for example, a ring of four sites like in Fig. 3: in order to minimize the energy of bonds 2, 3, 4 all four spins must be parallel, but then the energy of bond 1 is $|J_{BB}|$,

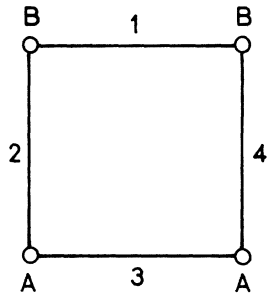


FIG. 3. Four-site ring in which the energies of all bonds cannot be minimized simultaneously.

not $-|J_{BB}|$. We can conclude from this example that (a) our approximation should not be trusted at very low temperatures, where the existence of closed loops imposes constraints which we are not taking into account; and (b) the exact ground-state energy lies between the Bethe-Peierls and mean-field energies at $T=0$. Mean-field theory completely neglects the correlations between neighboring spins, thus overestimating the ground-state energy, and the opposite is true for Bethe-Peierls theory. A more detailed analysis reveals that for $kT > \min(J_{AB}, |J_{BB}|)$, the neglect of closed loops is not a serious error. It can be checked in all the examples of Sec. V that $\min(J_{AB}, |J_{BB}|)$ is well below the bicritical or tetracritical point, so that this limitation does not invalidate our arguments.

## IV. DISCUSSION OF THE SELF-CONSISTENCY EQUATIONS

In this section we discuss the solutions of Eqs. (12) around the lines $OA, OB$ of Fig. 1, where the magnetizations are small and the right hand sides can be expanded in powers of the $u$'s. We set the external field $h=0$.

As mentioned before, there always exists a paramagnetic solution $u_A = u'_A = u_B = u'_B = 0$. Moreover it is clear on physical grounds that this must be the only solution at high $T$. According to the implicit-function theorem, a second solution may appear in the vicinity of $u_A = u'_A = u_B = u'_B = 0$ only if the Jacobian

$$g = \frac{\partial(\phi_A, \phi'_A, \phi_B, \phi'_B)}{\partial(u_A, u'_A, u_B, u'_B)} \tag{15}$$

vanishes at the origin [we have set $\phi_A \equiv u_A - f_A(u_A, u'_A, u_B, u'_B)$, etc.]. The lines $OA, OB$ of Fig. 1 correspond to second-order transitions; an ordered solution with small $u$'s exists immediately beneath these lines. Therefore *along* these lines $g$ must vanish. Calculating the Jacobian explicitly and writing $\tanh(\beta J_{ii'}) \equiv t_{ii'}$ for brevity we get

$$g = \left(\frac{\gamma-1}{\gamma}\right)^4 \begin{vmatrix} (\gamma-1)^{-1} & -c_A t_{AA} & 0 & -c_B t_{AB} \\ -c_A t_{AA} & (\gamma-1)^{-1} & -c_B t_{AB} & 0 \\ 0 & -c_A t_{AB} & (\gamma-1)^{-1} & -c_B t_{BB} \\ -c_A t_{AB} & 0 & -c_B t_{BB} & (\gamma-1)^{-1} \end{vmatrix}$$

$$= \left[\left(\frac{1}{\gamma-1} - c_A t_{AA}\right)\left(\frac{1}{\gamma-1} - c_B t_{BB}\right) - c_A c_B t_{AB}^2\right]$$

$$\times \left[\left(\frac{1}{\gamma-1} + c_A t_{AA}\right)\left(\frac{1}{\gamma-1} + c_B t_{BB}\right) - c_A c_B t_{AB}^2\right], \tag{16}$$

and the lines $OA, OB$ can be obtained by setting the last line equal to zero. It is easily verified that the line $OA$ is obtained when the first pair of square brackets is equated to zero, and similarly for the line $OB$ with the second pair. The easiest way to plot the curves is to solve for $c_A$ or $c_B$; the problem then reduces to solving a second-order algebraic equation with coefficients depending on $T$. We have thus found the boundary between the paramagnetic phase and the phases with long-range order.

To make further progress it is convenient to follow Wegner[6] and carry out a linear transformation to diagonalize the Jacobian, Eq. (16). Let

$$\lambda_{1,2} = \tfrac{1}{2}\{c_A t_{AA} + c_B t_{BB} \pm [(c_A t_{AA} - c_B t_{BB})^2 + 4 c_A c_B t_{AB}^2]^{1/2}\} \tag{17}$$

be the eigenvalues of the Hermitian matrix

$$M = \begin{pmatrix} c_A t_{AA} & (c_A c_B)^{1/2} AB \\ (c_A c_B)^{1/2} AB & c_B t_{BB} \end{pmatrix} \tag{18}$$

and

$$\begin{pmatrix} \cos\theta \\ \sin\theta \end{pmatrix} \quad \begin{pmatrix} -\sin\theta \\ \cos\theta \end{pmatrix} \tag{19}$$

be the corresponding eigenvectors. We define new variables $m, n, m', n'$ by

$$m = \frac{u_A + u'_A}{c_A^{1/2}} \cos\theta + \frac{u_B + u'_B}{c_B^{1/2}} \sin\theta, \tag{20a}$$

$$n = -\frac{u_A + u'_A}{c_A^{1/2}} \sin\theta + \frac{u_B + u'_B}{c_B^{1/2}} \cos\theta, \tag{20b}$$

$$m' = \frac{u_A - u'_A}{c_A^{1/2}} \cos\theta + \frac{u_B - u'_B}{c_B^{1/2}} \sin\theta, \tag{20c}$$

$$n' = -\frac{u_A - u'_A}{c_A^{1/2}} \sin\theta + \frac{u_B - u'_B}{c_B^{1/2}} \cos\theta. \tag{20d}$$

From the signs it is clear that the variables $m, n$ are associated with ferromagnetic order, the $m'$, $n'$ with antiferromagnetic order. Rewriting Eqs. (12) in terms of the new variables one gets

$$m\left(\lambda_1-\frac{1}{\gamma-1}\right)+P_m=0, \tag{21a}$$

$$n\left(\lambda_2-\frac{1}{\gamma-1}\right)+P_n=0, \tag{21b}$$

$$m'\left(-\lambda_1-\frac{1}{\gamma-1}\right)+P_{m'}=0, \tag{21c}$$

$$n'\left(-\lambda_2-\frac{1}{\gamma-1}\right)+P_{n'}=0, \tag{21d}$$

where the various $P$'s are homogeneous polynomials of degree 3 in $m,n,m',n'$ [we have expanded Eqs. (12) up to fourth order in the $u$'s]. It is easily verified that along the line $OA$, Fig. 1, $\lambda_1=1/(\gamma-1)$, so if a nontrivial solution exists around this line it must have $m\sim|\lambda_1-1/(\gamma-1)|^{1/2}$ and $m',n,n'$ of order $m^3\ll m$. Similarly in the neighborhood of $OB$, $\lambda_2\sim-1/(\gamma-1)$, $n'\sim|\lambda_2+1/(\gamma-1)|^{1/2}$, and $m,m',n$ are negligible compared to $n'$. Since in both cases $n$ and $m'$ are negligible we set them equal to zero right from the beginning, and retain only Eqs. (21a) and (21d).

The next step is to find $P_m$ and $P_{n'}$ explicitly in order to actually solve the two equations (21a) and (21d). Some lengthy algebra, which we omit, leads to

$$m(A+Bm^2+Cn'^2)=0, \tag{22a}$$

$$n'(D+Fm^2+Gn'^2)=0, \tag{22b}$$

with

$$A=\lambda_1-1/(\gamma-1), \tag{23a}$$

$$B=\frac{1}{12}\left(\frac{\cos^4\theta}{c_A}+\frac{\sin^4\theta}{c_B}\right)(\lambda_1^3-\lambda_1)+\frac{t_{AB}\sin\theta\cos\theta}{4(c_Ac_B)^{1/2}}[(t_{AA}-\lambda_1c_A)\cos^2\theta+(t_{BB}-\lambda_1c_B\sin^2\theta)]$$
$$-\frac{\lambda_1}{4}\left(t_{AA}\frac{c_B}{c_A}\cos^4\theta+t_{BB}\frac{c_A}{c_B}\sin^4\theta\right), \tag{23b}$$

$$C=\frac{\sin^2\theta\cos^2\theta}{4c_Ac_B}(\lambda_2^2-1)\lambda_1+\frac{t_{AB}\sin\theta\cos\theta}{4(c_Ac_B)^{1/2}}[\lambda_1-(t_{AA}\sin^2\theta+\lambda_1c_A\cos^2\theta)-(t_{BB}\cos^2\theta+\lambda_1c_B\sin^2\theta)]$$
$$+\frac{\lambda_1}{4}\sin^2\theta\cos^2\theta\left(t_{AA}\frac{c_B}{c_A}+t_{BB}\frac{c_A}{c_B}\right), \tag{23c}$$

$$D=-\lambda_2-1/(\gamma-1), \tag{23d}$$

$$F=\frac{\sin^2\theta\cos^2\theta}{4c_Ac_B}\lambda_2(1-\lambda_1^2)+\frac{t_{AB}\sin\theta\cos\theta}{4(c_Ac_B)^{1/2}}[(t_{AA}\cos^2\theta+\lambda_2c_A\sin^2\theta)+(t_{BB}\sin^2\theta+\lambda_2c_B\cos^2\theta)-\lambda_1]$$
$$+\frac{\lambda_2}{4}\sin^2\theta\cos^2\theta\left(t_{AA}\frac{c_B}{c_A}+t_{BB}\frac{c_A}{c_B}\right), \tag{23e}$$

$$G=\frac{1}{12}\left(\frac{\sin^4\theta}{c_A}+\frac{\cos^4\theta}{c_B}\right)(\lambda_2-\lambda_2^3)+\frac{t_{AB}\sin\theta\cos\theta}{4(c_Ac_B)^{1/2}}[(\lambda_2c_A-t_{AA})\sin^2\theta+(\lambda_2c_B-t_{BB})\cos^2\theta]$$
$$-\frac{\lambda_2}{4}\left(t_{AA}\frac{c_B}{c_A}\sin^4\theta+t_{BB}\frac{c_A}{c_B}\cos^4\theta\right). \tag{23f}$$

We conclude that the solutions can be classified into four types:

$$m=n'=0 \text{ (paramagnetic)}, \tag{24a}$$

$$m^2=-A/B,\quad n'=0 \text{ (ferromagnetic)}, \tag{24b}$$

$$m=0,\quad n'^2=-D/G \text{ (antiferromagnetic)}, \tag{24c}$$

$$m^2=\frac{DC-AG}{BG-FC},\quad n'^2=\frac{AF-BD}{BG-FC} \text{ (mixed)}. \tag{24d}$$

When more than one real solution exists one must compare the free energies in order to choose the one that is physically correct. This comparison can be done as follows: let $m^{(1)}(T),n'^{(1)}(T)$ and $m^{(2)}(T),n'^{(2)}(T)$ be two solutions of (22) and $E^{(1)}(T)$ and $E^{(2)}(T)$ the corresponding energies, Eq. (13). The two solutions can be followed up to $T_c$, the critical temperature, where they must merge into the trivial solution $m=n'=0$. From the thermodynamic identity $\partial(F/T)/\partial T=-E/T^2$ it follows that

$$F^{(1)}(T)-F^{(2)}(T)=T\int_T^{T_c}\frac{E^{(1)}(T)-E^{(2)}(T)}{T^2}dT. \tag{25}$$

Since the integrand can be computed at all temperatures between $T$ and $T_c$ our problem is solved. To construct the phase diagrams presented below we have compared the free energies of the various

solutions by computing the integral (25) numerically in all cases.

## V. COMPARISON WITH MEAN-FIELD SAMPLE CALCULATIONS

In the mean-field approximation the environment of each spin is replaced by an average medium, and this is then determined self-consistently. Wegner[6] found in this approximation a set of equations identical to our (22) but with the constants $A$, $B$, $C$, $D$, $F$, and $G$ different from our (23). We briefly sketch an alternative derivation of the mean-field equations.

Consider an $A$ atom on $L$; this atom is surrounded on the average by $\gamma c_A A$ atoms and by $\gamma c_B B$ atoms, all in $L'$. Calling $\sigma_A$, $\sigma_B$, $\sigma'_A$, and $\sigma'_B$ the average magnetizations, the effective field seen by an $A$ on $L$ is therefore $h_{\text{eff}}^{(A)} = \gamma c_A J_{AA} \sigma'_A + \gamma c_B J_{AB} \sigma'_B$, so that one of the equations is

$$\sigma_A = \tanh[\beta(\gamma c_A J_{AA} \sigma'_A + \gamma c_B J_{AB} \sigma'_B)], \tag{26a}$$

and similar equations for $A \leftrightarrow B$ and for $L \leftrightarrow L'$:

$$\sigma_B = \tanh[\beta(\gamma c_A J_{AB} \sigma'_A + \gamma c_B J_{BB} \sigma'_B)], \tag{26b}$$

$$\sigma'_A = \tanh[\beta(\gamma c_A J_{AA} \sigma_A + \gamma c_B J_{BB} \sigma_B)], \tag{26c}$$

$$\sigma'_B = \tanh[\beta(\gamma c_B J_{AB} \sigma_A + \gamma c_B J_{BB} \sigma_B)]. \tag{26d}$$

The whole analysis of Sec. IV can be repeated to arrive again at Eqs. (22), but now

$$A = \lambda_1 - 1, \tag{27a}$$

$$B = -\frac{\lambda_1^3}{12}\left(\frac{\cos^4\theta}{c_A} + \frac{\sin^4\theta}{c_B}\right), \tag{27b}$$

$$C = -\left(\frac{\lambda_1 \lambda_2^2}{4 c_A c_B}\right) \sin^2\theta \cos^2\theta, \tag{27c}$$

$$D = -\lambda_2 - 1, \tag{27d}$$

$$F = \left(\frac{\lambda_1^2 \lambda_2}{4 c_A c_B}\right) \sin^2\theta \cos^2\theta, \tag{27e}$$

$$G = \frac{\lambda_2^3}{12}\left(\frac{\sin^4\theta}{c_A} + \frac{\cos^4\theta}{c_B}\right), \tag{27f}$$

and $\lambda_1, \lambda_2, \theta$ are now obtained from the matrix

$$\begin{pmatrix} c_A J_{AA} \gamma / kT & (c_A c_B)^{1/2} J_{AB} \gamma / kT \\ (c_A c_B)^{1/2} \gamma J_{AB} / kT & c_B J_{BB} \gamma / kT \end{pmatrix}. \tag{28}$$

We have investigated the phase diagrams around the point $O$, Fig. 1, for several values of the coupling constants, using the Bethe-Peierls and mean-field equations. All results are for coordination number $\gamma = 6$.

Figure 4 shows a typical case of weak coupling between the species: $J_{AA} = 1$, $J_{BB} = -0.5$, and $J_{AB} = 0.4$. It is known that mean-field results overestimate the critical temperature, and the Bethe-Peierls results are somewhat lower as was to be expected. Otherwise the agreement is quite good.

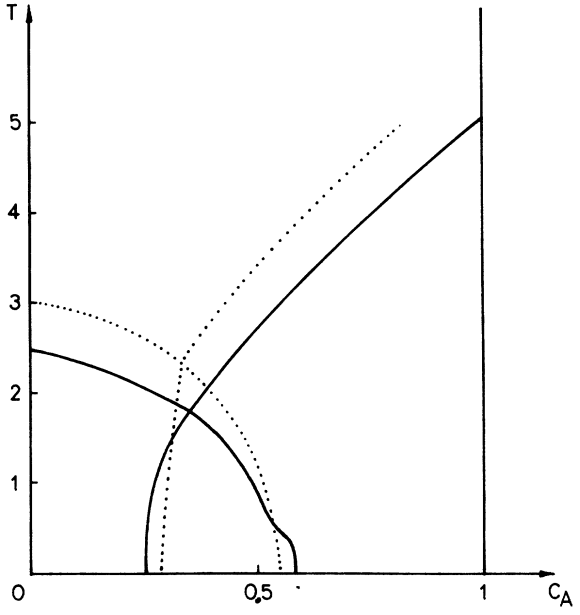


FIG. 4. Phase diagram for weak interspecies coupling: $J_{AA} = 1$, $J_{BB} = -0.5$, $J_{AB} = 0.4$, and $\gamma = 6$. Full line: Bethe-Peierls; dotted line: mean field.

To illustrate the properties of the various phases we have plotted in Fig. 5 the magnetizations of the two types of atoms on each of the sublattices at a fixed concentration $c_A = 0.45$. The results were obtained with the Bethe-Peierls equations and the coupling constants are the same as in the previous case. The total magnetization of sublattice $L$ is related to the curves by $\langle\sigma\rangle = c_A\langle\sigma_A\rangle + c_B\langle\sigma_B\rangle$ and similarly for $L'$. One can see that for $T < T_1$ the magnetizations $\langle\sigma\rangle$ and $\langle\sigma'\rangle$ are neither equal nor opposite, and this corresponds to a mixed state. For temperatures between $T_1$ and $T_2$ the magnetizations on $L$ and $L'$ are the same; the order is ferromagnetic.

Figure 6 shows the energy vs concentration for the same system at various temperatures. Zones with different type of order are separated by dotted lines. The discontinuities in the slope of $E$ across the boundaries are consistent with second-order transitions.

In Fig. 7 we have a case of intermediate coupling between species: $J_{AA} = 1, J_{BB} = -0.5, J_{AB} = 1$. For these coupling constants we get in our approach a tetracritical point and a mixed phase; molecular field results instead predicts a bicritical point with a first-order AFM-FM line. Apparently as $J_{AB}$ is increased the mixed state disappears less easily than predicted by mean-field theory.

For a strong coupling between species, $J_{AA} = 1$,

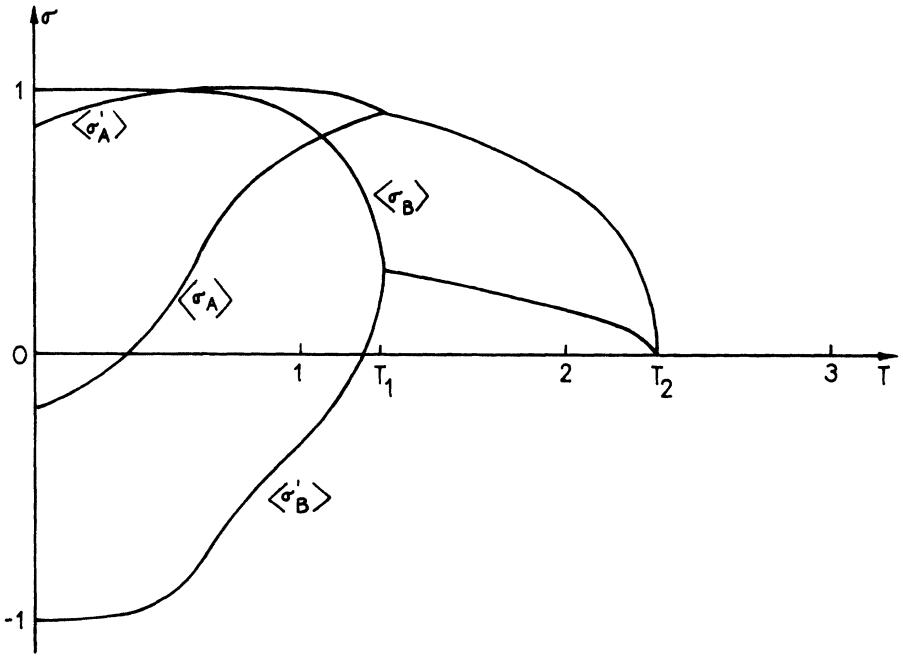


FIG. 5. Magnetization of $A$ and $B$ spins on sublattices $L$ and $L'$ for $c_A = 0.45$ and same coupling constants as in Fig. 5. The total magnetizations of the sublattices are $\langle\sigma\rangle = c_A\langle\sigma_A\rangle + c_B\langle\sigma_B\rangle$ and $\langle\sigma'\rangle = c_A\langle\sigma'_A\rangle + c_B\langle\sigma'_B\rangle$. The system is in the mixed state for $T < T_1$ and in the ferromagnetic state for $T_1 < T < T_2$.

$J_{BB} = -0.5, J_{AB} = 2$, there is again qualitative agreement between the two approximations; both give a first-order line as shown in Fig. 8.

Finally we shall comment on the $T = 0$ behavior of the alloy. We have not been able to obtain an analytic solution of Eqs. (12) in the limit $T \to 0$, but for the simpler mean-field equations this limit is readily studied. For $T \to 0$ the hyperbolic tangents in Eqs. (26) go to $\pm 1$, and after a few consistency checks one finds the following three possibilities:

$$\sigma_A = \sigma'_B = 1, \quad \sigma_B = \sigma'_A = -1 \quad \text{(AFM)}$$

$$\text{for } c_A < \frac{J_{AB}}{J_{AA} + J_{AB}}, \tag{29a}$$

$$\sigma_A = \sigma_B = \sigma'_A = 1, \quad \sigma'_B = -1 \quad \text{(mixed)}$$

$$\text{for } \frac{J_{AB}}{J_{AA} + J_{AB}} < c_A < \frac{|J_{BB}|}{J_{AB} + |J_{BB}|}, \tag{29b}$$

$$\sigma_A = \sigma_B = \sigma'_A = \sigma'_B = 1 \quad \text{(FM)}$$

$$\text{for } \frac{|J_{BB}|}{J_{AB} + |J_{BB}|} < c_A. \tag{29c}$$

If $J_{AB} < (J_{AA}|J_{BB}|)^{1/2}$ the region of validity of (29b) is nonempty and the phases at $T = 0$ are AFM-mixed-FM in order of increasing $c_A$. If, on the contrary, $J_{AB} > (J_{AA}|J_{BB}|)^{1/2}$ no mixed phase exists. Comparison of the energies shows that in this case the AFM is stable for $c_A < |J_{BB}|^{1/2}/(J_{AA}^{1/2} + |J_{BB}|^{1/2})$, the FM beyond this point.

An interesting fact, apparently not noticed before, is the following: the condition for the existence of a mixed state at $T = 0$,

$$J_{AB} < (J_{AA}|J_{BB}|)^{1/2}, \tag{30}$$

is compatible with a bicritical point at $O$, Fig. 1. Thus, phase diagrams like Fig. 9 are predicted by

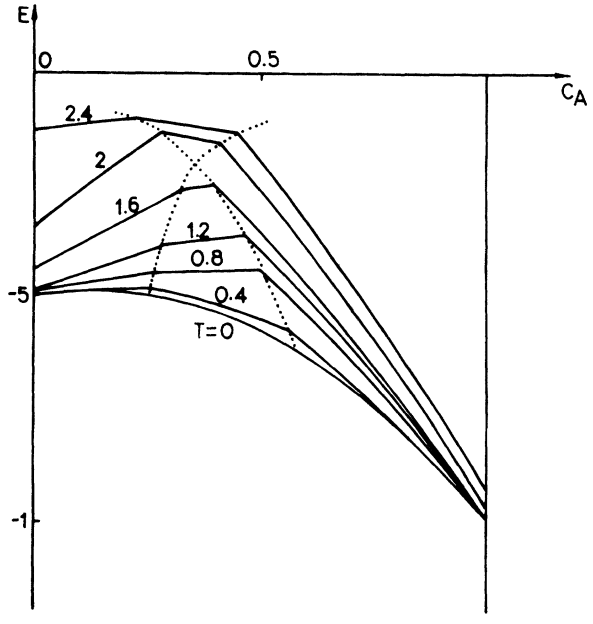


FIG. 6. Energy vs concentration at several temperatures for the same coupling constants as in Figs. 4 and 5. The dotted line separates phases and corresponds to the full line in Fig. 4.

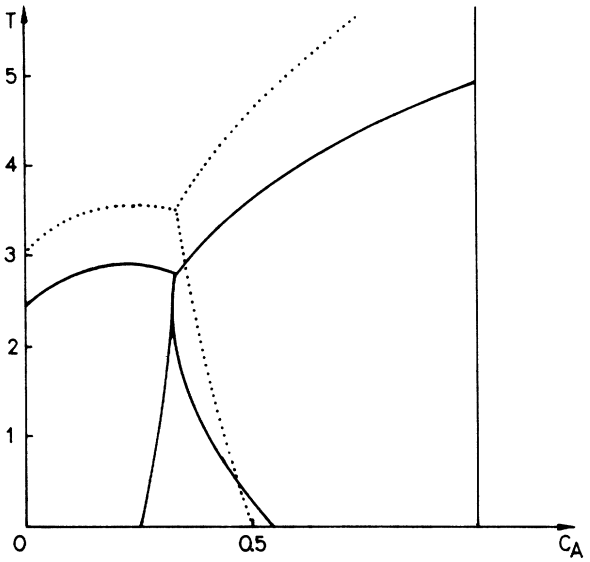


FIG. 7. Phase diagram for intermediate coupling: $J_{AA}=1$, $J_{BB}=-0.5$, $J_{AB}=1$. The Bethe-Peierls approximation (full line) predicts a mixed phase separated from the ferromagnetic and antiferromagnetic phases by second-order transitions. Mean-field approximation (dotted line) instead gives a first-order line and no mixed state.

mean-field theory for certain values of the coupling constants (an example is $J_{AA}=2, J_{BB}=-0.5, J_{AB}=0.95$). We have made no attempt at a systematic investigation of the solutions of (12) for $T=0$ because, as explained at the end of Sec. III, the solutions cannot be trusted anyway at very low $T$. Nevertheless, the following result seems worth mentioning: in the calculations for Fig. 8 we have seen, in addition to the first-order line, a small

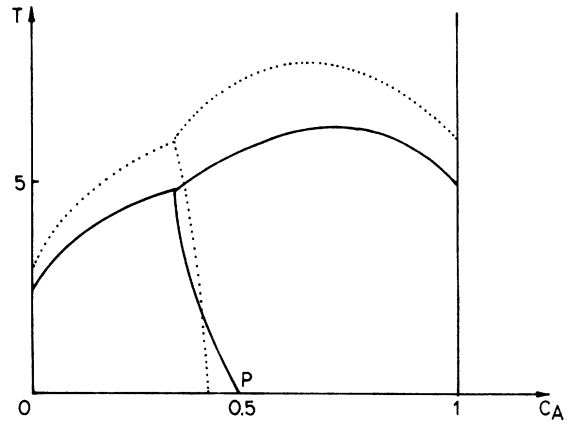


FIG. 8. Phase diagram for strong interspecies coupling: $J_{AA}=1$, $J_{BB}=-0.5$, $J_{AB}=2$. Both theories predict a line of first-order transitions.

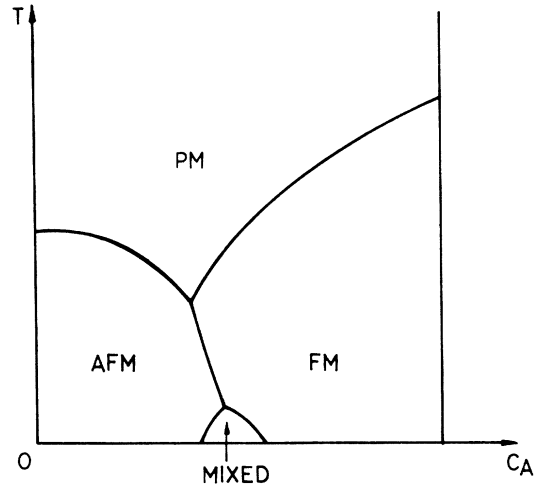


FIG. 9. Another type of phase diagram predicted by mean-field theory.

region around point $P$ in which the system is in a mixed state. This region has a triangular shape, extending from $c_A \sim 0.32$ to $c_A \sim 0.55$ on the $T=0$ line and has its upper vertex on the first-order line at $T \sim 0.6$. Within our numerical accuracy (better than 0.1%) the energy is perfectly smooth across the boundary of this region; the magnetizations are continuous with a discontinuous slope.

As mentioned earlier, at $T=0$ the exact solution is somewhere between the mean-field and Bethe-Peierls approximations because the first completely neglects correlations between neighboring spins while the second overestimates them. Both approximations predict phase diagrams which at very low $T$ are more complicated than Fig. 1. This strongly suggests that there actually is some complication around $T=0$ in the exact phase diagram.

On the other hand, the existence of a tetracritical or bicritical point (point $O$, Fig. 1), depending on the strength of the interspecies coupling $J_{AB}$, is a result which can be believed with reasonable confidence; both approximations agree quite well on this point.

## VI. SUMMARY

We have extended the Bethe-Peierls approximation to a system in which two types of order, ferromagnetic and antiferromagnetic, may exist. This constitutes a refinement over previous mean-field calculations. Mean-field theory predicts two different kinds of phase diagrams: (a) For strong coupling between the species ($J_{AB}$ large), Fig. 1(a) results. There are three phases with a line of first-order transitions separating the AFM from the FM phase. (b) For weak coupling (small $J_{AB}$)

a fourth mixed phase appears as shown in Fig. 1(b). The mixed phase arises from the interpenetration of a dilute ferromagnet (the $A$ atoms) with a dilute antiferromagnet (the $B$ atoms).

Our Bethe-Peierls results are more accurate than mean-field results, since bigger clusters are considered exactly. We obtain phase diagrams with all critical lines shifted to lower temperatures, as it should be since mean-field theory is known to overestimate $T_c$. But, more important than this quantitative improvement, is the fact that our results confirm the qualitative predictions of mean field theory, thereby strengthening our confidence in the whole picture.

Some anomalies in the very-low-$T$ region suggest that the phase diagram may show additional complications at $T \sim 0$.

---

*Work supported in part by CONICET, Argentina.

[1]S. C. Brush, Rev. Mod. Phys. 39, 883 (1967).
[2]C. Fan and B. McCoy, Phys. Rev. 182, 614 (1969).
[3]F. T. Lee, E. W. Montroll, and Lee-po Yu, J. Stat. Phys. 8, 309 (1973).
[4]T. P. Eggarter, J. Stat. Phys. 11, 363 (1974).
[5]Ch. Wissel, Phys. Status Solidi B 51, 669 (1972).
[6]F. Wegner, Solid State Commun. 12, 785 (1973).
[7]A. D. Bruce and A. Aharony, Phys. Rev. B 11, 478 (1975).
[8]References to experimental work are given in Refs. 5 and 6.
[9]This restriction can be dropped without drastic changes in the formalism, simply by replacing the products $c_i c_{i'}$ in Eqs. (8) and those following by the corresponding pair probabilities.
[10]C. Domb, Adv. Phys. 9, 145 (1960).